Biochemical and Biophysical Research Communications 452 (2014) 895–900

Contents lists available at ScienceDirect

Biochemical and Biophysical Research Communications

journal homepage: www.elsevier.com/locate/ybbrc

# Synergistic contribution of SMAD signaling blockade and high localized cell density in the differentiation of neuroectoderm from H9 cells

Chao Liu [a,b,c,*], Yaping Sun [b], Joshua Arnold [d], Bingwei Lu [c], Su Guo [b,*]

[a] Department of Histology and Embryology, Institute of Stem Cell and Tissue Engineering, Anhui Medical University, Hefei, Anhui 230032, China
[b] Department of Bioengineering and Therapeutic Sciences, University of California San Francisco, CA 94143, USA
[c] Department of Pathology, Stanford University School of Medicine, Stanford, CA 94305, USA
[d] Stem Cell Core, Gladstone Institute of Cardiovascular Disease, University of California San Francisco, San Francisco, CA 94158, USA

ARTICLE INFO

*Article history:*
Received 21 August 2014
Available online 10 September 2014

*Keywords:*
Localized cell density
Seeding cell density
Differentiation
Human embryonic stem cells
Neuroectoderm

ABSTRACT

Directed neural differentiation of human embryonic stem cells (ESCs) enables researchers to generate diverse neuronal populations for human neural development study and cell replacement therapy. To realize this potential, it is critical to precisely understand the role of various endogenous and exogenous factors involved in neural differentiation. Cell density, one of the endogenous factors, is involved in the differentiation of human ESCs. Seeding cell density can result in variable terminal cell densities or localized cell densities (LCDs), giving rise to various outcomes of differentiation. Thus, understanding how LCD determines the differentiation potential of human ESCs is important. The aim of this study is to highlight the role of LCD in the differentiation of H9 human ESCs into neuroectoderm (NE), the primordium of the nervous system. We found the initially seeded cells form derived cells with variable LCDs and subsequently affect the NE differentiation. Using a newly established method for the quantitative examination of LCD, we demonstrated that in the presence of induction medium supplemented with or without SMAD signaling blockers, high LCD promotes the differentiation of NE. Moreover, SMAD signaling blockade promotes the differentiation of NE but not non-NE germ layers, which is dependent on high LCDs. Taken together, this study highlights the need to develop innovative strategies or techniques based on LCDs for generating neural progenies from human ESCs.



## 1. Introduction

Generating desired cell types from human embryonic stem cells (ESCs) offers the potential of creating new cell sources for regenerative medicine [1–3]. To realize this potential, it is essential to precisely understand the role of various endogenous and exogenous factors involved in the differentiation of human ESCs [4–6].

Cell density is a factor taken into consideration but is still rather poorly understood. Normally, cell density indicates a specific number of cells in a total culture space, which is applicable only for the single-cell-based cell seeding method. For human ESCs, high density culturing generates central nervous system (CNS)-neuronal derivatives, while lower density conditions favor peripheral nervous system (PNS) development [6]. Nevertheless, high cell seeding densities is required for the final differentiation of pancreatic amylase-positive cells from human ESCs [7]. High density cultures also favor pancreatic progenitor commitment and an increased formation of pancreatic endocrine cell populations [5]. Thus, different differentiation protocols using human HESCs seeded at a high cell density result in the divergent outcomes of different germ layers, leaving an elusive question: how can human ESCs seeded at a high cell density give rise to desired outcomes during neural differentiation of human ESCs?

During human neural development, neuroectoderm (NE) differentiation is a key process that generates the primordium of the human nervous system [8,9]. Unless mechanisms involved in NE differentiation from human ESCs are elucidated, generating desired neural derivatives from human ESCs for regenerative medicine might only be a bench work that is far from clinical applications.

*Abbreviations:* ESC, embryonic stem cell; LCD, localized cell density; NE, neuroectoderm; CNS, central nervous system; PNS, peripheral nervous system; MEF, mouse embryonic fibroblasts; KSR, knockout serum replacement; FGF2, fibroblast growth factor 2; DAPI, 4,6-diamidino-2-phenylindole.

* Corresponding authors. Address: Department of Histology and Embryology, Institute of Stem Cell and Tissue Engineering, 81 Meishan Road, Anhui Medical University, Hefei, Anhui 230032, China (C. Liu). Address: Department of Bioengineering and Therapeutic Sciences, Programs in Human Genetics and Biological Sciences, University of California San Francisco, CA 94143, USA (S. Guo).

*E-mail addresses:* chaol1974@ahmu.edu.cn (C. Liu), su.guo@ucsf.edu (S. Guo).

http://dx.doi.org/10.1016/j.bbrc.2014.08.137
0006-291X/

Although cell seeding density plays a role in the differentiation of human ESCs into different germ layers, we cannot ignore that it is the terminal cell density or LCD that presents final outcomes of various differentiation experiments. Localized cell density (LCD), a niche property of human ESCs, is a function of the number of neighbors a cell has within a given space and has been proposed to play a role in the self-renewal and differentiation of human ESCs [10], highlighting the importance of examining LCD when optimizing human ESC neural differentiation protocols. However, the role of LCD in affecting NE differentiation from human ESCs still remains unclear.

In the present study, we attempted to address the importance of the role of localized rather than seeding cell density in the differentiation of NE from H9 human ESCs. We report the initially seeded cells form derived cells with variable LCDs and subsequently affect the NE differentiation. Using a newly developed method to quantitatively examine LCD, we showed that in the presence of induction medium supplemented with or without SMAD signaling blockers, high LCD contributes to the differentiation of NE. Further study indicated that SMAD signaling blockade facilitates the LCD-dependent differentiation of NE but not non-NE cells. Taken together, these results may indicate a need to develop highly efficient protocols based on LCD for H9 cell neural differentiation.

## 2. Materials and methods

### 2.1. Cell culture

The human ESC line H9 has been previously described [11,12]. The cells were propagated weekly on Matrigel (BD Bioscience, Bedford, MA) in mTeSR medium (Stem Cell Technologies, Vancouver, BC, Canada) or on irradiated mouse embryonic fibroblasts (MEFs, Chemicon) in human ESC medium consisting of Knockout-DMEM (Invitrogen, Carlsbad, CA), 0.1 mM β-mercaptoethanol (Sigma), 1 mM L-glutamine (Invitrogen), 1% non-essential amino acids (Invitrogen), 20% knockout serum replacement (KSR; Invitrogen), 1% penicillin streptomycin (Invitrogen), and 10 ng/ml human basic fibroblast growth factor (FGF2; R&D), as previously described [6]. The ESC medium was changed every day. A cell-clump-based method was performed according to the protocol from Stem Cell Company; the mTeSR medium was changed every day. The human ESCs were passaged using dispase (Stem Cell Technologies) and replated in mTeSR medium at a dilution of 1:6.

### 2.2. Neuroectoderm induction

Single cell-based differentiation of NE was performed as previously described [6]. Briefly, H9 cells were cultured on MEFs in KSR medium (DMEM/F12, 20% KSR, 0.1 mM β-mercaptoethanol, 10 ng/ml of FGF-2) and disaggregated using accutase (Millipore, Billerica, MA, USA) for 20 min, washed with KSR medium and pre-plated on gelatin-coated 6-well plates for 1 h at 37 °C in the presence of the ROCK inhibitor (Y-27632) to remove MEFs. The nonadherent human ESCs were washed and plated on a Matrigel-coated 6-well plate at a density of 4000–20,000 cells/cm$^2$ in MEF-conditioned KSR medium with 10 ng/ml FGF-2 and ROCK inhibitor. The ROCK inhibitor was withdrawn the next day, and the human ESCs were allowed to expand in the mTeSR medium for 3 days or until the cells were nearly confluent. For the cell-clump-based differentiation of NE, human ESCs cultured on Matrigel in mTeSR medium were passaged with dispase and replated on a Matrigel-coated 6-well plate at a dilution of 1:3 in mTeSR medium. The human ESC clumps were allowed to expand in mTeSR medium for 3 days or until the cells were nearly confluent. Next, the clumps were subjected to NE induction. NE induction medium is a combination of the KSR medium and N2 medium (DMEM/F12, 1% N2 supplement, 10 ng/ml FGF2, 0.1 mM mercaptoethanol). The amount of N2 medium was increased (25%, 50%, 75%, and 100%) with the induction. The derived cells were subjected to an IF assay on the 5th day and were harvested and subjected to an RT-PCR assay on the 6th day. For SMAD signaling blockade, the NE induction medium was supplemented with 10 μM SB431542 (S) (Tocris) and 500 ng/ml of NOGGIN (N) (Sigma) for the indicated times. N2 medium supplemented with 0.2 mM AA (ascorbic acid, Sigma) was used for prolonged differentiation until d11.

### 2.3. Immunofluorescence (IF) assay

The IF assay was performed as previously described [13]. Cells cultured on Matrigel-coated coverslips were fixed using 4% paraformaldehyde for 20 min, washed with PBS, permeabilized using 0.1% Triton X-100 in PBS and blocked with 0.1% FBS in PBS. Antibodies used for immunofluorescence analysis were as follows: mouse anti-Oct4 (Santa Cruz, 1:500), rabbit anti-PAX6 (1:1000, Covance), mouse anti-PAX6 (1:400; Millipore), rabbit anti-PAX6 (1:200, Millipore), rabbit anti-NESTIN (Sigma, 1:1000), and mouse anti-beta-III-tubulin (1:200) (Millipore). An Axioobserver Z1 (Zeiss) microscope and a NIKON Eclipse 80I fluorescence microscope were used for microscopy. The nuclei were counterstained with 4,6-diamidino-2-phenylindole (DAPI).

### 2.4. RT-PCR

Human ESCs or derived cells were harvested for total RNA isolation using an RNA isolation KIT (Axygen). For RT-PCR analysis of mRNAs, 1 μg of total RNA from each sample was reverse transcribed with Superscript III (Invitrogen). Next, 10% of the first-strand reaction (2 μl) was used for subsequent PCRs for each gene of interest, with a GAPDH endogenous control used for normalization. PCR primers for the markers have been previously described [14]. The sequences of the primers and the size of the PCR products are shown in Table 1.

### 2.5. Immunoblotting (IB) assay

An immunoblotting (IB) assay was performed as previously described [15]. Antibodies used for IB were as follows: monoclonal rabbit anti-OCT4 (1:500, Santa Cruz), rabbit anti-PAX6 (1:500, Millipore), mouse anti-beta-III-tubulin (1:500, Millipore), and rabbit anti-GAPDH (1:5000, Ptglab).

### 2.6. Statistics

To evaluate the differences in protein levels, Image J software was used. The relative expression of OCT4 and PAX6 among the

**Table 1**
Primer sequences of markers used for RT-PCR analysis. The size of each PCR product is shown.

| Primer | Sequence | Size (bp) |
|---|---|---|
| OCT4 | 5′-AGTGAGAGGCAACCTGGAGA-3′<br>5′-GTGAAGTGAGGGCTCCCATA-3′ | 273 |
| PAX6 | 5′-AACAGACACAGCCCTCACAAACA-3′<br>5′-CGGGAACTTGAACTGGAACTGAC-3′ | 275 |
| GAPDH | 5′-GTACTCAGCGCCAGCATCG-3′<br>5′-AGCCACATCGCTCAGACACC-3′ | 302 |
| BRACHYURY | 5′-CTTCCCTGAGACCCAGTTCAC-3′<br>5′-CAGGGTTGGGTACCTGTCAC-3′ | 289 |
| GATA2 | 5′-AGCCGGCACCTGTTGTGCAA-3′<br>5′-TGACTTCTCCTGCATGCACT-3′ | 242 |

total cells was calculated based on the areas in the OCT4, PAX6 and DAPI (4,6-diamidino-2-phenylindole) channels. Differences in cell numbers were evaluated based on the number of positive cells for PAX6 and DAPI. Statistical analysis was performed using one-way ANOVA, and the data are presented as the mean ± SD.

## 3. Results

### 3.1. Cells with LCD showed direct differentiation outcomes in H9 cells

PAX6 is a NE determinant in humans [16]. Thus, we used PAX6 as a marker to monitor the differentiation of NE. We investigated PAX6 expression during the differentiation of H9 cells using a single-cell-based induction method. This method uses KSR and N2 medium supplemented with two blockers of SMAD signaling, namely NOGGIN and SB431542. H9 cells maintained on Matrigel in mTeSR medium were used as a control (Fig. 1A–D). Cells grown for 5 days in mTeSR medium generated cells with high LCDs (Fig. 1C). These cells were not PAX6-positive (Fig. 1 A and D) but were OCT4-positive (Fig. 1B and D). In contrast, KSR and N2 medium supplemented with NOGGIN and SB431542 induced PAX6 expression (Fig. 1 E, H, I and L), combined with a down-regulation of OCT4 (Fig. 1F, H, J and L). Unexpectedly, H9 cells plated at a lower density ($8 \times 10^3$ cells/cm$^2$) formed many cell masses in which most cells were PAX6-positive (Fig. 1E and H), while H9 cells plated at a higher density ($2 \times 10^4$ cells/cm$^2$) did not form PAX6-positive cell masses but demonstrated scattered PAX6-positive cells (Fig. 1I and L). Moreover, the PAX6-positive cell masses were characterized by higher LCDs compared to PAX6-negative cells (Fig. 1E and H, arrows). Statistical data of OCT4 and PAX6 signals in H9 cells and H9-derived cells indicated a significant increase in PAX6 expression, which was correlated with a significant decrease in OCT4 expression in a cell density-dependent manner (Fig. 1M).

Taken together, these results indicated that the initially seeded cells form derived cells with high LCDs first, and the derived cells subsequently affect PAX6 expression during the differentiation of the NE from H9 cells.

### 3.2. Quantitative examination of PAX6 expression in NE cells

To quantitatively examine LCD, we developed a new cell counting strategy, of which each micrograph was obtained with a resolution of 3840 × 3072 pixels (25 × 20 cm) and was divided into 20 (5 × 4) small squares (Fig. 2A–D). Each square has a limited area ($1.69 \times 10^{-4}$ cm$^2$) such that the LCD can be calculated by counting the number of cells within it. Because ESCs differentiated spontaneously under a confluent condition even in the presence of feeder cells, which might disrupt directed lineage specification [17], we plated H9 cells as small clumps for NE differentiation (Fig. 2). NESTIN, a neural stem cell marker that is also expressed at an earlier stage of neural differentiation, was used as a control. At day 6, both PAX6 and NESTIN were expressed in the derived cells (Fig 2A–D). Interestingly, the PAX6 expression was found to be highest in cells with high LCD (Fig. 2A and D), while NESTIN expression was found to be highest in cells with low LCD (Fig. 2B and D). The PAX6-positive, NESTIN-positive and DAPI-positive cells (Fig. 2B and D) in each square were quantified using Image J software. Regions with equivalent LCDs were binned together, and the average cell densities of different regions are shown (Fig. 2E). The ratio of PAX6 and

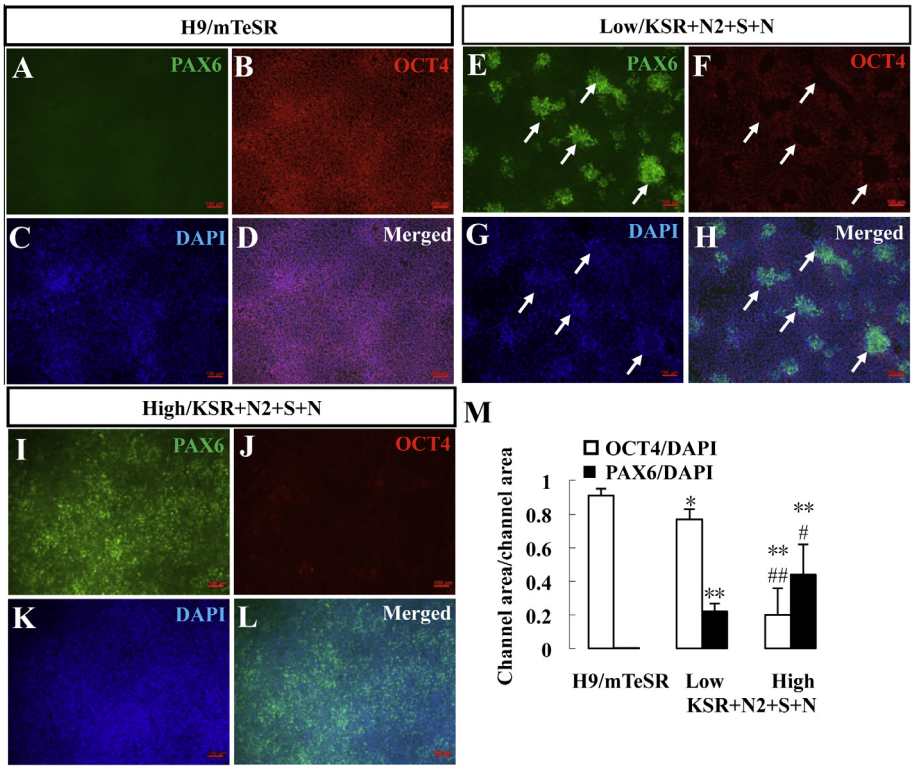


**Fig. 1.** LCD shows direct differentiation outcomes of H9 cells seeded at different densities. (A–D) Undifferentiated H9 cells with localized high cell density were subjected to IF using anti-PAX6 (A and D) and anti-OCT4 (B and D) antibodies. (E–L) H9 cells seeded at low density ($8 \times 10^3$ cells/cm$^2$) (E–H) and high density ($1 \times 10^4$ cells/cm$^2$) (I–L) were treated with KSR and N2 medium supplemented with NOGGIN and SB431542 for 5 days. The cells were then subjected to the IF assay using anti-PAX6 antibody (green, E, H, I and L) and anti-OCT4 antibody (red, F, H, J and L) in the H9-derived cells. (M) The areas of the signals in the OCT4, PAX6 and DAPI channels were calculated using Image J software. The ratios of the OCT4 and PAX6 area to DAPI area are shown (X ± SD, $n = 8$; $^{*}P < 0.05$; $^{**}P < 0.01$, compared with the H9 cells; $^{\#}P < 0.05$; $^{\#\#}P < 0.01$, compared with the low density, using one-way ANOVA with SPSS 17.0 software). (For interpretation of the references to color in this figure legend, the reader is referred to the web version of this article.)

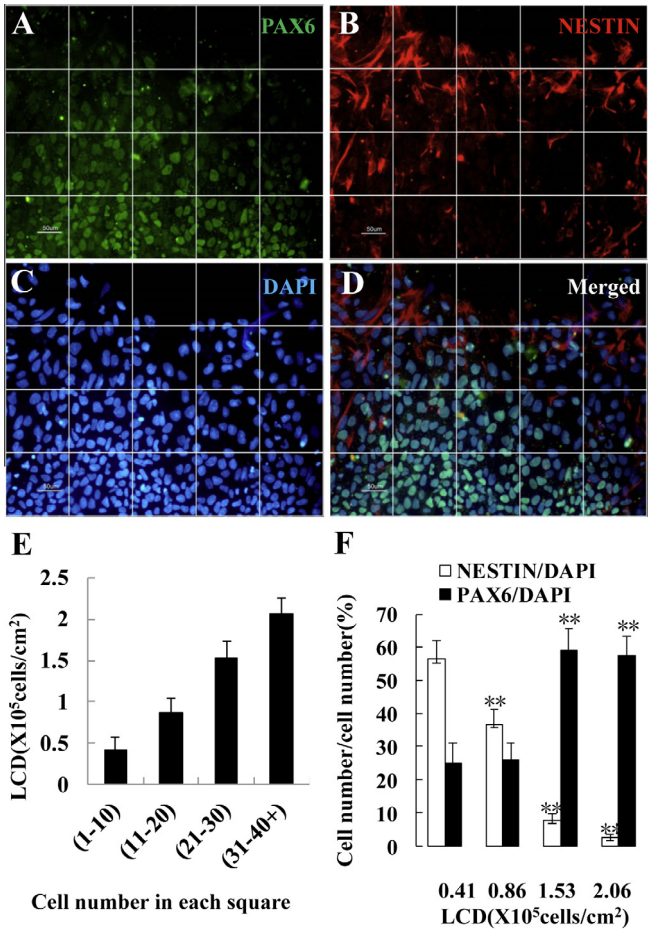


**Fig. 2.** Differential LCD-dependent expression of PAX6 and NESTIN during NE differentiation. (A–D) Cell-clump-based differentiation of NE was performed for 5 days. The cells were then subjected to the IF assay using anti-PAX6 (Fig. 2A and D) and anti-NESTIN (Fig. 2B and D) antibodies. A square-based cell quantification strategy was developed. Each micrograph with a resolution of 3840 × 3072 pixels was divided into 20 (5 × 4) squares (Fig. 2A–D). (E, F) Next, the PAX6-positive cells, NESTIN-positive cells and DAPI-positive cells in each square were quantified using Image J software. Regions with equivalent LCDs were binned together into five subgroups, and the average cell densities are shown (Fig. 2E). Statistical analyses were performed on the ratio of PAX6 and NESTIN to DAPI in the derived cells with different cell densities (Fig. 2F).

NESTIN to DAPI was subjected to statistical analysis (Fig. 2F). More than 50% NESTIN-positive cells were found in the lowest LCD region ($0.41 \times 10^5$ cells/cm$^2$). The ratio decreased with an increase in LCD and is less than 3% when the LCD reached the highest density ($2.06 \times 10^5$ cells/cm$^2$). In contrast, only 25% PAX6-positive cells were found in the lowest LCD region. When the LCD increased to a density of $1.53 \times 10^5$ cells/cm$^2$, the ratio of PAX6-positive cells increased significantly to 59%, which is similar to that of the cells in the highest LCD region. These results provide a quantitative evaluation that PAX6 expression in NE cells is LCD-dependent.

### *3.3. Quantitative evaluation of the synergistic contribution of LCDs and SMAD signaling blockade to NE differentiation*

To minimize the use of exogenous factors and to examine if LCD and SMAD signaling blockers have synergistic effects on NE differentiation, we next performed cell-clump-based differentiations of NE with or without the presence of NOGGIN and SB431542. Without the presence of NOGGIN and SB431542, PAX6 expression was also identified in H9-derived cells (Fig. 3A and B). Quantitative analysis indicated that high LCDs resulted in a significant increase in the number of PAX6-positive cells (Fig. 3E). The presence of

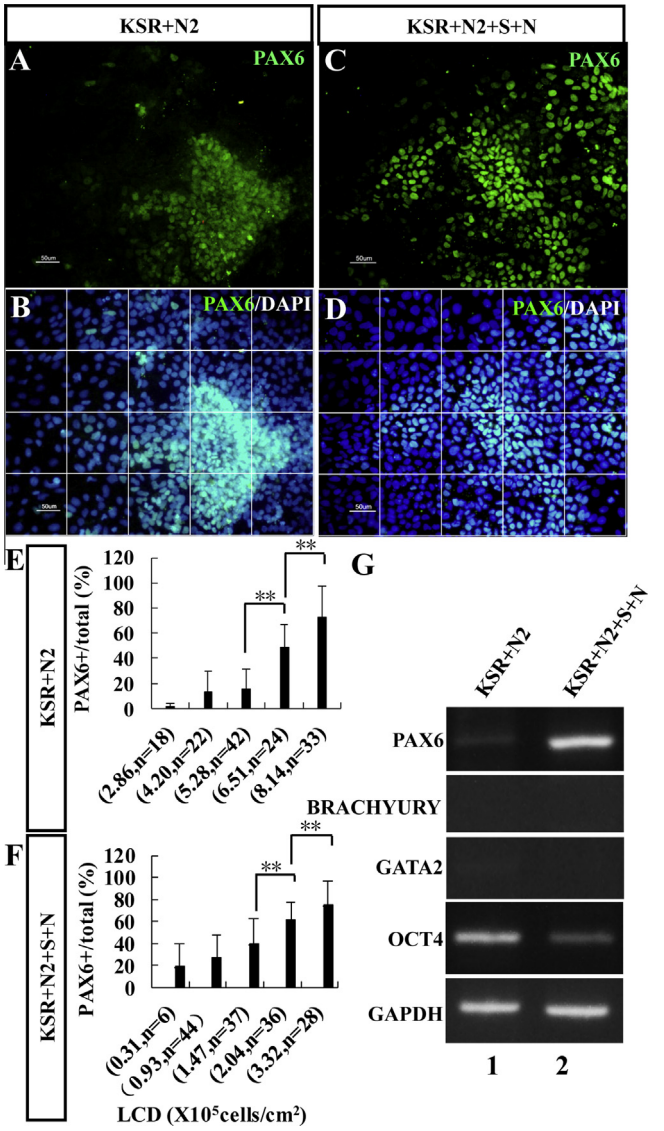


**Fig. 3.** Synergistic contribution of SMAD signaling blockers and localized high cell density in NE differentiation. (A–F) Five days after the cell-clump-based differentiation of NE in KSR and N2 medium with (D–F) or without (A–C) SMAD signaling blockers, H9-derived cells were subjected to the IF assay using anti-PAX6 antibody (green, A–D). The nuclei were stained using DAPI (blue, C and D). The micrographs were divided into 20 (5 × 4) squares as indicated (C and D). (E–F) The number of total cells and PAX6-positive cells in each square was quantified using Image J software. The ratio of PAX6-positive cells to total cells in each square was determined. The squares with equivalent ratios were binned together. The ratios of PAX6-positive cells to total cells in each bin are shown ((F) X ± SD, $^{**}P < 0.01$, using one-way ANOVA with SPSS 17.0). (G) Cell-clump-based differentiation of NE was performed with (lane 2) or without (lane 1) NOGGIN and SB431542. On the 6th day of differentiation, the H9-derived cells were harvested and subjected to RT-PCR assays for the indicated marker genes. OCT4, a pluripotent marker; PAX6, a human NE determinant; BRACHYURY, a mesoendoderm marker; GATA2, a non-NE marker. (For interpretation of the references to color in this figure legend, the reader is referred to the web version of this article.)

NOGGIN and SB431542 promoted NE differentiation by increasing the number of PAX6-positive cells even in cells with relatively low LCDs (Fig. 3F). RT-PCR assays also demonstrated that NOGGIN and SB431542 decreased OCT4 and increased PAX6 mRNA levels. In contrast, weak or no mRNA expression of BRACHYURY and GATA2, two non-NE markers [3,18], was detected despite the presence of NOGGIN and SB431542 (Fig. 3G).

These results quantitatively indicated that high LCD is one of the endogenous parameters that cooperates with SMAD signaling blockers, thereby contributing to the differentiation of NE.

### 3.4. Expression of marker proteins in H9 cells and H9-derived neural cells

To further examine the neuronal differentiation potential of NE cells, H9 cells and H9-derived cells were harvested at different time points and subjected to IB for the indicated markers. Robust expression of OCT4 was detected in H9 cells, while OCT4 expression in the H9-derived cells was found to significantly decrease at d5 and disappeared at d10. PAX6 expression was upregulated during differentiation and peaked at d5, followed by a downregulation at d10. Beta-III-tubulin, a neuronal cell marker, was upregulated during differentiation and reached its highest expression at d10 (Fig. 4A). Downregulation of OCT4 expression at d5 was demonstrated using the IF assay (Fig. 4B). Upregulation of beta-III-tubulin was also shown using the IF assay (Fig. 4C and D).

## 4. Discussion

The promise of human ESCs in regenerative medicine is dependent on their potential to generate diverse neural cell populations [19]. Both endogenous and exogenous factors are involved in regulating human ESC neural differentiation [20]. When cultured in NE induction medium supplemented with SMAD signaling blockers, H9 cells seeded at different densities showed differential expression of PAX6-positive cells, which was correlated with the different LCDs (Fig. 1E–H and I–L), indicating that different seeding cell densities resulted in cells with variable LCDs, which finally induce variable expression of PAX6 in NE cells. H9 cells are characterized by growth in cell clumps with different sizes [17]. We also demonstrated that H9 cells plated as single cells at different cell densities resulted in cell clumps with variable sizes (Supplement Fig. 1). Thus, we propose that in addition to seeding cell density, terminal cell density or LCD is also one of the endogenous factors required during neural differentiation of human ESCs.

Using a newly established strategy for the quantitative examination of LCD, it is possible to obtain a quantitative understanding of the role of LCDs in the expression of PAX6 in NE cells. Differential LCD-dependent expression of PAX6 and NESTIN was subsequently observed (Fig. 2). Expression of PAX6 is upregulated with an increase in LCD (Fig. 2A–F). Thus, we used PAX6 as an indicator to investigate the synergistic contribution of LCDs and SMAD signaling blockers in the differentiation of NE cells. Although the expression of PAX6 is also LCD-dependent (Fig. 3A, B and E), in the absence of SMAD signaling blockers, the NE differentiation efficiency significantly decreased. SMAD signaling blockers increased NE differentiation efficiency by decreasing the cell density required for PAX6 induction (Fig. 3C, D and F). RT-PCR assays also confirmed the contribution of SMAD signaling blockers in the expression of PAX6 but not non-NE marker genes (Fig. 3G).

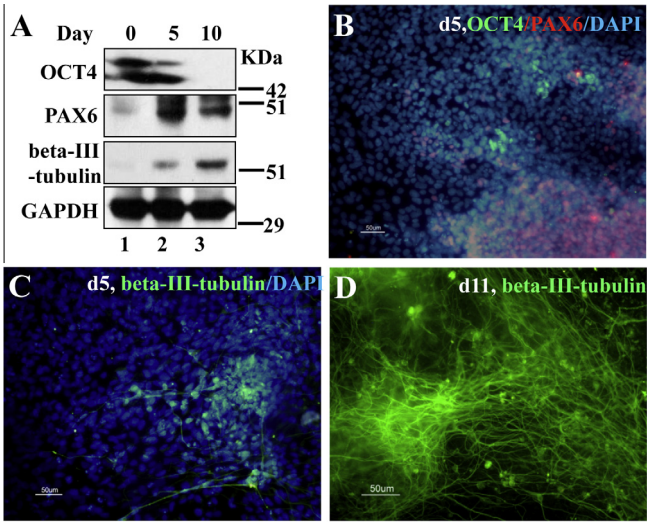


**Fig. 4.** Expression of neuronal marker proteins in the derived neuronal cells. (A) H9-derived cells were subjected to the IB assay using the indicated antibodies at different time points of the cell-clump-based H9 differentiation. The undifferentiated H9 cells were used as a control. (B–D) H9-derived cells were subjected to the IF assay for the indicated marker proteins. Beta-III-tubulin, a neuronal marker.

Using the IB assay, downregulation of OCT4 and upregulation of PAX6 were confirmed (Fig. 4A), which were consistent with the IF assay and RT-PCR assay results. Moreover, using both the IF assay and IB assay, the expression of beta-III-tubulin was found to increase with differentiation (Fig. 4A, C and D), suggesting the generation of more neuronal cells. These data support the idea that generating H9 cells with high LCDs may be a better way to differentiate NE compared to average or overall high cell densities. Because human ESCs are maintained routinely as cell clumps [17], it may be difficult to specify various LCDs only according to seeding cell density. Recently, a Matrigel-dependent patterning technique, which enables a method resembling the cell-clump-based plating method, has been used to study mechanisms involved in human ESC self-renewal and differentiation[21]. Further studies using similar technique may provide an understanding of the optimal tight control of LCDs for the neural induction of H9 cells. Finally, cell density is only one of the various factors involved in the neural differentiation of human ESCs. It has been combined with other factors, such as growth factors [7], colony and aggregate size [10], expansion time [22], seeding protocol [23] and matrix concentration [24], to play a crucial role in the differentiation of various stem cells, including the neural differentiation of human ESCs. Thus, it also remains to be elucidated how cell density, particularly LCD, cooperates with other factors involved in NE induction to generate optimal outcomes.

Taken together, our data may be a step forward to focus on the role of high LCD in the differentiation of NE, which may contribute to the development of highly efficient protocols for the generation of neural derivatives from human ESCs.

## Acknowledgments

Our research project was sponsored by a grant from the National Natural Science Foundation of the People's Republic of China (31271159), a Technology Foundation for Selected Overseas Chinese Scholar (2012 No.13) Grant from Anhui HRSS, a Grant for scientific research of BSKY (XJ201105) from Anhui Medical University, and the following Grants: NIH NIDA R01 DA023904 and CIRM GUO-RS1-00215-1. The funding agencies had no role in the study design, data collection and analysis, decision to publish, or preparation of the manuscript.

## Appendix A. Supplementary data

Supplementary data associated with this article can be found, in the online version, at http://dx.doi.org/10.1016/j.bbrc.2014.08.137.

## References

[1] O. Lindvall, Z. Kokaia, Stem cells in human neurodegenerative disorders – time for clinical translation?, J Clin. Invest. 120 (2010) 29–40.
[2] D.E. Cohen, D. Melton, Turning straw into gold: directing cell fate for regenerative medicine, Nat. Rev. Genet. 12 (2011) 243–252.
[3] M. Thomson, S.J. Liu, L.N. Zou, Z. Smith, A. Meissner, S. Ramanathan, Pluripotency factors in embryonic stem cells regulate differentiation into germ layers, Cell 145 (2011) 875–889.
[4] H. Kumagai, H. Suemori, M. Uesugi, N. Nakatsuji, E. Kawase, Identification of small molecules that promote human embryonic stem cell self-renewal, Biochem. Biophys. Res. Commun. 434 (2013) 710–716.

[5] B.K. Gage, T.D. Webber, T.J. Kieffer, Initial cell seeding density influences pancreatic endocrine development during in vitro differentiation of human embryonic stem cells, PLoS One 8 (2013) e82076.
[6] S.M. Chambers, C.A. Fasano, E.P. Papapetrou, M. Tomishima, M. Sadelain, L. Studer, Highly efficient neural conversion of human ES and iPS cells by dual inhibition of SMAD signaling, Nat. Biotechnol. 27 (2009) 275–280.
[7] S. Takizawa-Shirasawa, S. Yoshie, F. Yue, A. Mogi, T. Yokoyama, D. Tomotsune, K. Sasaki, FGF7 and cell density are required for final differentiation of pancreatic amylase-positive cells from human ES cells, Cell Tissue Res. 354 (2013) 751–759.
[8] T.J. Petros, J.A. Tyson, S.A. Anderson, Pluripotent stem cells for the study of CNS development, Front. Mol. Neurosci. 4 (2011) 30.
[9] C.E. Murry, G. Keller, Differentiation of embryonic stem cells to clinically relevant populations: lessons from embryonic development, Cell 132 (2008) 661–680.
[10] R. Peerani, B.M. Rao, C. Bauwens, T. Yin, G.A. Wood, A. Nagy, E. Kumacheva, P.W. Zandstra, Niche-mediated control of human embryonic stem cell self-renewal and differentiation, EMBO J. 26 (2007) 4744–4755.
[11] K.N. Ivey, A. Muth, J. Arnold, F.W. King, R.F. Yeh, J.E. Fish, E.C. Hsiao, R.J. Schwartz, B.R. Conklin, H.S. Bernstein, D. Srivastava, MicroRNA regulation of cell lineages in mouse and human embryonic stem cells, Cell Stem Cell 2 (2008) 219–229.
[12] Y. Yao, B. Nashun, T. Zhou, L. Qin, S. Zhao, J. Xu, M.A. Esteban, X. Chen, Generation of CD34+ cells from CCR5-disrupted human embryonic and induced pluripotent stem cells, Hum. Gene Ther. 23 (2012) 238–242.
[13] C. Liu, Y. Zhong, A. Apostolou, S. Fang, Neural differentiation of human embryonic stem cells as an in vitro tool for the study of the expression patterns of the neuronal cytoskeleton during neurogenesis, Biochem. Biophys. Res. Commun. 439 (2013) 154–159.
[14] S. Erceg, S. Lainez, M. Ronaghi, P. Stojkovic, M.A. Perez-Arago, V. Moreno-Manzano, R. Moreno-Palanques, R. Planells-Cases, M. Stojkovic, Differentiation of human embryonic stem cells to regional specific neural precursors in chemically defined medium conditions, PLoS One 3 (2008) e2122.
[15] L. Liu, C. Liu, Y. Zhong, A. Apostolou, S. Fang, ER stress response during the differentiation of H9 cells induced by retinoic acid, Biochem. Biophys. Res. Commun. 417 (2012) 738–743.
[16] X. Zhang, C.T. Huang, J. Chen, M.T. Pankratz, J. Xi, J. Li, Y. Yang, T.M. Lavaute, X.J. Li, M. Ayala, G.I. Bondarenko, Z.W. Du, Y. Jin, T.G. Golos, S.C. Zhang, Pax6 is a human neuroectoderm cell fate determinant, Cell Stem Cell 7 (2010) 90–100.
[17] J.A. Thomson, J. Itskovitz-Eldor, S.S. Shapiro, M.A. Waknitz, J.J. Swiergiel, V.S. Marshall, J.M. Jones, Embryonic stem cell lines derived from human blastocysts, Science 282 (1998) 1145–1147.
[18] M.A. Spinner, L.A. Sanchez, A.P. Hsu, P.A. Shaw, C.S. Zerbe, K.R. Calvo, D.C. Arthur, W. Gu, C.M. Gould, C.C. Brewer, E.W. Cowen, A.F. Freeman, K.N. Olivier, G. Uzel, A.M. Zelazny, J.R. Daub, C.D. Spalding, R.J. Claypool, N.K. Giri, B.P. Alter, E.M. Mace, J.S. Orange, J. Cuellar-Rodriguez, D.D. Hickstein, S.M. Holland, GATA2 deficiency: a protean disorder of hematopoiesis, lymphatics, and immunity, Blood 123 (2014) 809–821.
[19] S. Erceg, M. Ronaghi, M. Stojkovic, Human embryonic stem cell differentiation toward regional specific neural precursors, Stem Cells 27 (2009) 78–87.
[20] A.J. Keung, S. Kumar, D.V. Schaffer, Presentation counts: microenvironmental regulation of stem cells by biophysical and material cues, Annu. Rev. Cell Dev. Biol. 26 (2010) 533–556.
[21] C.L. Bauwens, R. Peerani, S. Niebruegge, K.A. Woodhouse, E. Kumacheva, M. Husain, P.W. Zandstra, Control of human embryonic stem cell colony and aggregate size heterogeneity influences differentiation trajectories, Stem Cells 26 (2008) 2300–2310.
[22] J.Y. Ko, J.Y. Lee, C.H. Park, S.H. Lee, Effect of cell-density on in-vitro dopaminergic differentiation of mesencephalic precursor cells, NeuroReport 16 (2005) 499–503.
[23] S.H. McBride, M.L. Knothe Tate, Modulation of stem cell shape and fate A: the role of density and seeding protocol on nucleus shape and gene expression, Tissue Eng. Part A 14 (2008) 1561–1572.
[24] V.S. Nirmalanandhan, M.S. Levy, A.J. Huth, D.L. Butler, Effects of cell seeding density and collagen concentration on contraction kinetics of mesenchymal stem cell-seeded collagen constructs, Tissue Eng. 12 (2006) 1865–1872.